THE ANNALS OF "DUNAREA DE JOS" UNIVERSITY OF GALATI.
FASCICLE IX. METALLURGY AND MATERIALS SCIENCE
N$^0$. 1 – 2008, ISSN 1453 – 083X

# XRD ANALYSIS IN FRONT OF A CORROSION CRACK TIP

**C. GHEORGHIEŞ, S. LEVCOVICI, V. PĂUNOIU, L. GHEORGHIEŞ, C. OANCEA, I. OSTACHE, P. ALEXANDRU**
"Dunarea de Jos" University of Galati, Romania
email:cgheorg@ugal.ro

## ABSTRACT

*During exploitation of the heat exchangers some damages can appear in the contact region between the gaskets and the stainless steel walls. The studies upon the material were performed using SEM microscopy, X-ray diffractometry and the finite element method. The obtained data allow the explanation of the complex damage mechanism of the heat exchanger wall. Following our research, the manufacturing technology of the heat exchangers was changed and this way the rebuts were eliminated. The performed research is based upon physical methods and the damage mechanism of the heat exchanger plates is explained by means of the physical phenomena that appear and develop during working conditions.*

KEYWORDS: stainless steel, structure, corrosion, crack, SEM, XRD.

## 1. Introduction

The aim of our research was to study the causes that led to the deterioration by cracking of the heat exchanger plates from some power stations. According to their technical documentation, the SCPW0.35 heat exchanger plates have a working temperature span between -10 degrees Celsius and + 150 degrees Celsius, at a maximum pressure of 1.6 MPa. The supplier of the product doesn't give any information concerning the material and its manufacturing technology. This is contrary to the data that other producers give concerning the material they used to make similar products, such as Alfa Laval Thermal (producing AISI 316, AISI 304, AISI 316L). The lifespan mentioned for their products in their documents is about 30 years. The beneficiary of the SCPW 0.35 products found out that the effective work regime of them agrees with the one specified by the producer, keeping into account that the primary agent didn't surpass $120^0$ C and 4 bar pressure. Working into steps, the temperature difference between the primary and the secondary agent from the heat exchanger is sensitively smaller than working separately. The chemical composition of both the primary and the secondary agents was in normal limits. Cracks appeared without exception at the inlet of the primary agent (hot water) in the exchanger, in areas below the tightening gasket, there where no one expects to have any mechanical overstress.

This is why it was necessary to conduct a deep study of both the material and the technology used for the making of SCPW 0.35 heat exchanger plates. The steps of our study are: a computer simulation of the technological process of drawing of the plates, thus finding out the residual tensions following the plates' processing. It also studied on the computer the possible development and propagation of cracks due to purely mechanical causes, meaning the residual tension forces from processing. It is studied what happens to the plates when they are processed by cold plastic deformation, by taking into consideration the elastic turning back of the material (the so-called spring back). Then, we performed the chemical composition of the material, a metallographic analysis, a microhardness analysis and X-ray diffraction fine structure analysis [1], by comparing our results with some aspects concerning the corrosion under stress process. The investigated samples were taken from its proximity, but also from unaffected areas situated at the inlet of the secondary agent. The study will be continued by analyzing the behavior of the material of the heat exchangers made by other firms, maybe on samples taken from semi fabricated, before processing, in order to make comparisons and to give recommendations to the makers.

## 2. Computer simulation

The general simulation [2, 3] is called "the method of the finite element" and it is capable of a three-dimensional study of deformations.

It consists of more steps:

1) the geometrical profiles for both the die-block (the underlining plate), for the underlining punch and for the semi-fabricated plate used for deformation are generated.

2) all the generated elements are divided into a finite number of small parts.

3) the simulation parameters are introduced like the geometrical model and some specific parameters. 4) the simulation is performed and conclusions are drawn concerning the three-dimensional distribution of the values of several important physical parameters.

There are two deformation models for the analysis of the pressing process, a simplified one and a complex one. According to the simplified model, a small area of the sample is analyzed, such that the shape of the semi fabricated is a plane plate and the basic geometrical elements are a rib and a circular area corresponding to the corner where the breaking appears. The geometrical elements of the complex simulation model consist of 24 ribs placed symmetrically around the circular area where the tightening gaskets are placed. This is the area where the cracks appeared. The shape of the semi fabricated is now circular, with an inlet that is close to the shape of the corresponding area of the real semi fabricated used to make the heat exchangers.

Before starting the simulations we made measurements in order to determine the precise shapes and sizes of the profiles that form the piece, especially into those areas where the cracks appeared. According to these measurements we could establish the coordinates of the points of a characteristic profile, containing the ribs and the areas where the in-between plates gaskets are placed.

The specific parameters used for the simulation were:

1) 0.11 friction coefficients between the semi-fabricated and the active elements;

2) 5.5 mm punch run, according to the depth of the gasket's place;

3) We considered a hypothetical hardening curve of the material because we didn't have a sample of the initial semi-fabricated material from which we could get an experimental curve of this kind;

4) The other data referring to the material, such as the Poisson coefficient, the density and the modulus of elasticity where taken equal to the ones for steel.

We can see in figure 1 the complex geometrical model in the simulation position. After an 80 hours running program, we could get a complex simulation, starting with 2500 elements and finishing with 67852 elements because of the automatic remaking of the finite elements net.

This model offers a better approach to the real plastic deformation than the simplified one.

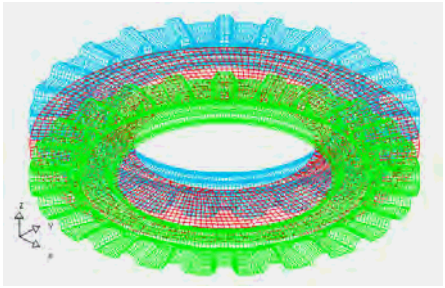

***Fig.1** The complex geometrical model in the simulation position*

Its results are shown in the following maps with specifically colored scales.

In figure 2 we can see the lack of uniformity of the thickness of our processed material. Even so, the thickness variations are rather small.

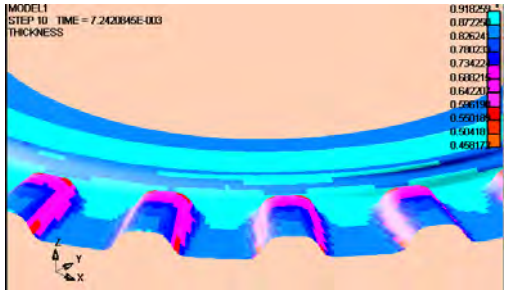


***Fig. 2.** The thickness variation of the material*

The variation of the radial tension is presented in figure 3.

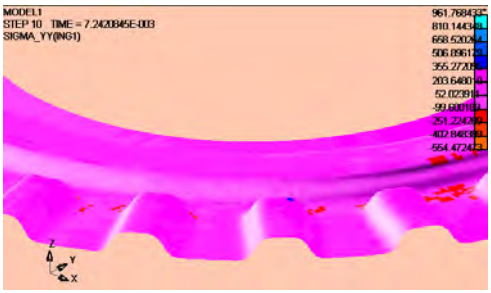


***Fig.3**. The variation of the radial tension*

According to the values obtained for the radiate tensions, disposed perpendicular to the cracks, we could conclude that as it is normal, stretching tensions around 300 MPa appear at the edge of the gaskets' area, close to the outlet, in the middle of the material. In the lower part, the tensions are also of stretching type, with the same kind of values. In the upper part we have compression tensions, so that a bending effect emerges. The normal circumferential tensions are compression-type on the entire thickness and breadth of the fixing gaskets' area.

We came to the conclusion that the stress state for an individual element is close to a pure shearing state,

with a tangential tension close to the modulus of radiate and circumferential tensions. So, there is a possibility that cracks appear in a zigzag shape, such as we could really notice at a close exam of the affected areas.

The distribution of the Von Mises flow tensions is presented in figure 4, according to the Von Mises flow criterion, when the plastic state is attained if the value of the flow resistance surpasses the value given by the next formula:

$$\sqrt{2}\cdot\sigma_c = \sqrt{(\sigma_1-\sigma_2)^2+(\sigma_2-\sigma_3)^2+(\sigma_3-\sigma_1)^2} \qquad (1)$$

where $\sigma_1$, $\sigma_2$, $\sigma_3$ are the normal principal tensions and $\sigma_c$ is the flow limit of the material [1].

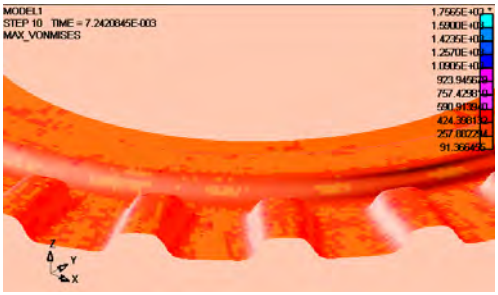


***Fig. 4.*** *The distribution of the Von Mises flow tensions*

From this last simulation it was concluded that the tensions that appear during the deformation process cannot represent a real cause for cracking of the heat exchanger plates [2, 4].

## 3. The experimental analysis of the cracked plates

The samples used for the metallographic and diffraction analysis were taken both from the cracked area, where the hot fluid enters and also from the uncracked areas, corresponding either to the exit of the hot fluid, either from the circulation of the heated fluid [5, 6].

***Fig. 5.*** *Uncracked area of the heat exchanger*

It is interesting to notice that cracks appear every time at the inlet area of the hot thermal agent (the hottest area) and also on the plane portion of the rib that serves as the place for the tightening gaskets between the neighboring plates.

We can see clear corrosion traces of the piece's surface on the cracked area. These traces do not appear on the rest on the surface, which is also in contact with the same working fluid.

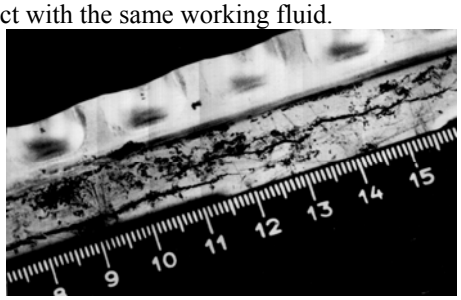


***Fig. 6.*** *A cracked area of the heat exchanger*

The drawing of the samples was done by manual blade cutting such that the influence of the samples' detachment to be minimum. It was noticed that cutting the samples in the cracked area leads to the breaking of the surface in almost distinct pieces, even though cracks cannot be seen on the sample. This phenomenon was noticed even when drawing the samples from the very proximity of the cracked area, proving that the material was much more affected by cracks than it can be observed with the naked eye. A simple strain made by friction of the saw blade's cutting edges in these areas leads to the breaking into pieces of the surface. This aspect wasn't noticed when drawing samples from the uncracked (uncorroded) corners. We used the same drawing method of samples destined for metallographic and X-ray diffraction analysis. The results of our analysis are as it follows.

### *3.1 Chemical analysis*

The determination of composition was performed by spectral method on the samples taken from the uncorroded part of the plate analyzed. The chemical composition of the investigated material is presented in table 1 according to the chemical analysis bulletin, emitted from the Mix Foundry Laboratory of MITTAL STEEL Company Galati, Romania. The niobium content was also checked by chemical analysis, according to the trial report, emitted from the Central Laboratory – MITTAL Steel Company Galati, Romania.

The thermal treatment recommended by STAS 3583-80 is hardening from $1050^0$ C until $1100^0$ C, followed by cooling in air, oil or water.

The chemical analysis points out that a stainless steel unstabilized with titanium or niobium being unstable in sulfur environments and having an oxidation temperature of 800 degrees Celsius of AISI 304 type (12NiCr180 STAS-ISO 3583-80 mark) for pieces used in corrosive media is recommended.

***Table 1.*** *Chemical composition of samples*

| | Analyzed material | | | |
|---|---|---|---|---|
| | **Elements** | **Sample** | **AISI 304** | **12NiCr180** |
| **Chemical composition (%)** | C | 0.05 | Max 0.08 | Max 0.12 |
| | Mn | 0.38 | Max 2 | Max 2 |
| | Si | 0.87 | Max 1 | Max 1 |
| | P | 0.029 | 0.030 | - |
| | S | 0.026 | 0.045 | - |
| | Al | 0.014 | - | - |
| | Cu | 0.05 | - | - |
| | Cr | 18.70 | 18-20 | 17-19 |
| | Ti | 0.005 | - | - |
| | Ni | 8.24 | 8-12 | 8-10 |
| | V | 0.04 | - | - |
| | W | 0.04 | - | - |
| | Nb | 0.011 | - | - |

### *3.2. Metallographic analysis*

As it can be seen in figure 7, the samples were included in a teeth-type of acrylate in order to analyze them in cross-section. We prepared the samples for analyzis by buffing, polishing and electrolytically attacking them in a 50 % solution of nitric acid.

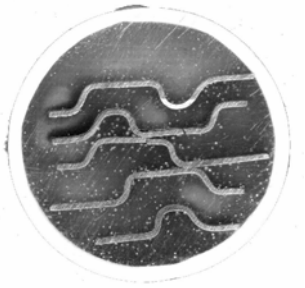

***Fig. 7.*** *Sample preparation for metallographic analysis*

We performed the metallographic analysis at × 100 and ×500 increases, on the Neophot microscope, from the Material Science Laboratory of "Dunarea de Jos" University of Galati. This analysis on the polished samples proved the presence of more nonmetallic inclusions distributed into rows along the rolling line. We could also see in the samples some plastic formations of sulphures (see fig.8).

The electrolytically attacked samples have a microstructure made of thin austenitic grains with 8-point granularity, according to STAS 5490-80, with thin inter-grain precipitates of carbides (See fig. 9 and 10).

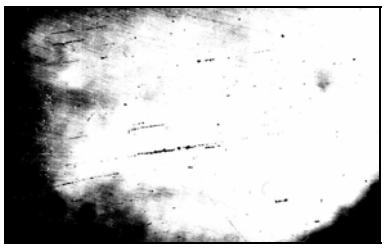

***Fig. 8.*** *Nonmetallic inclusions*

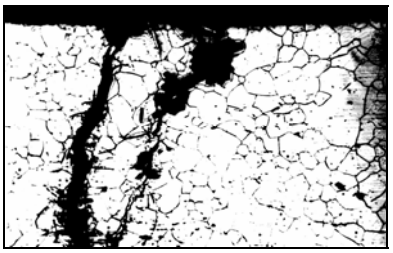

***Fig. 9.*** *Transcrystalline crack (attacked sample; 500 ×)*

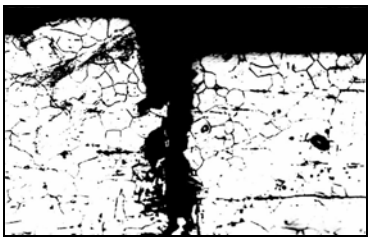

***Fig. 10.*** *A crack and nonmetallic inclusions (500 ×)*

### *3.3. Microhardness analysis*

The microhardening analyses were performed in the cross-section of more cracked areas of two metallographic samples with different degrees of plastic deformation [7]. The samples were taken both from the crosscut direction and the planar faces of the rib where the gaskets are placed (see the sketch from below, in fig. 11). During the cold plastic deformation there is a high degree of deformation in the cross-rib, while in the plane-face of the rib the deformation is lower. We determined the $HV_{0.1}$ Vickers microhardness [daN/mm$^2$], at 100 grams load, according to STAS (ISO) 7657-78, at a PMT3-type of microhardness device from the Material Science Laboratory, as above. We found out at one of the samples the microhardness at 0.05 mm distance from the surface of the metal sheet, on its outline, in order to observe the hardening of the fibers that were stretched or compressed during the plastic deformation process. In figure 11 we present the values of the $HV_{0.1}$ Vickers microhardness in daN/mm$^2$ and the measuring points of the microhardness [8].

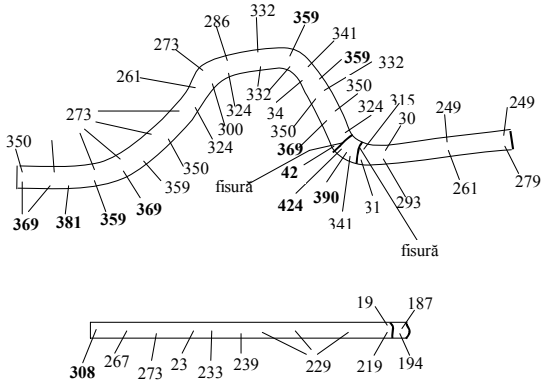


***Fig. 11.** The experimental variation of the Vickers microhardness in diverse points.*

The characteristics of the sample with a complex profile and high degree of cold plastic deformation made for the relatively big pieces are as it follows:

1) The microhardness is relatively high compared with the one of the sample with a simpler profile.

2) The maximum hardness in the neighborhood of the cracks begun on the stretched fiber of the profile indicates the hardening is an encouraging factor for cracking.

3) During the cold plastic deformation of the plates' profile, the stretched fibers have a higher hardness than the compressed fibers. These stretched fibers are areas preferred for the cracks to begin.

4) The left edge area is hardened during the cutting of the initial metal sheet from which the heat exchanger plates were made.

5) The right edge area of the sample that breaks during use is softened because of the relaxation of the breaking tension forces.

The sample with a lower degree of plastic deformation during plates' making has a much lower microhardness. This fact proves both the relaxation of the stress state in the neighborhood of the cracks and the growth of the microhardness in the cold plastically deformed area.

The concerning literature[2] indicates that the global hardening results, during the cold plastic deformation (rolling and/or drawing) of the austenitic stainless steel, because of several special factors:

1) partial change of the austenite to martensite;

2) hardening of the formed martensite.

The elasticity limit of the steel is raised from 30 daN/mm$^2$ to 100 daN/mm$^2$ by a 50 % metal covering at ambient temperature of a stainless steel with 18 % Cr and 8 % Ni. Thus, the steel becomes less able to be processed by cold plastic deformation.

## 4. Theoretical aspects concerning the corrosion process

It was studied the electrochemical corrosion and the corrosion under mechanical stress of the heat exchangers' material.

### *4.1. Electrochemical corrosion and the influence of the microstructure upon it*

The potential difference from a galvanic cell with electrochemical corrosion [9, 11] can be generated by a variety of causes that produce the heterogeneity of the metallic material or that of the electrolyte, such as:

1) differences between the chemical composition between the anode and the cathode;

2) differences in the state of residual or applied stress forces;

3) differences in the chemical composition of the electrolyte. According to these causes, the corresponding galvanic cells with electrochemical corrosion are classified into 3 classes: composition cells; elastic distortion cells and concentration cells, respectively.

At the heat exchanger plates, the chemical analysis shows an allied steel type AISI 304. External producers like Alfa Lava Thermal use for the heat exchanger plates both the 304 AISI steel for less aggressive media, and 1316 AISI steel with <0.08 % C; <2 % Mn; maximum 0.03 % S, maximum 0.045 % P, 16 – 18 % Cr; 10 – 14 % Ni and 2 – 3 % Mo. Meanwhile, ZILMET uses the 316L AISI steel, with carbon content less than 0.03 percent.

The 304 AISI steel doesn't contain molybdenum that has an increased role of corrosion resistance into wet media, into reducing agents and into chlorine media. Also, the low quantity of nickel from the steel of 8.24 % compared to minimum 10 % at 316 or 316L steel marks, decreases both the corrosion resistance into non oxidizing or weakly oxidizing media and the heat resistance of the steel.

The 304 AISI steel has higher carbon content than the 316L AISI steel. This favors, in the absence of enough Ti or Nb as stabilizing elements (Ti=5×C; Nb=10×C), a higher sensitivity to the apparition of carbides into the austenitic structure.

The microstructural analysis shows an inaccurate elaboration because of the observed big quantity of nonmetallic inclusions.

Because the exploitation temperature under 150$^0$ C doesn't lead to the precipitation of the carbides, we are probably talking about an unfit or absent thermal treatment of solving the carbides.

The presence of carbides and nonmetallic inclusions increases the chemical heterogeneity of the steel and its sensitivity to the apparition of the galvanic composition cells.

A worse condition for the corrosion is the local cover with corrosion products (rust or weak adherent oxides), because these products limit the access of oxygen. Thus, the covered metallic material becomes anodic and corrodes more and more. This is a pitting-type of corrosion and has the effect of a drastic cut-off of the lifetime of the metallic construction compared to the general corrosion that is characterized by the loss of weight.

In the case of the heat exchanger plates, the constructive solution of the exchanger activates a galvanic cell of differentiated aeration because of the aeration difference between the portion of the plate that is covered nonadherently with the gaskets, and the free surface that is in contact with the fluid. Thus, the visual and the microscopic analysis showed that the cracks began near the gaskets and then propagated into the area covered by the gaskets. There is also a potential difference due to the concentration difference between the primary and the secondary fluid on the two faces of the plate because of their different temperatures and pressures. The covering with cathodic products as rust of the face that is in contact with the hot fluid and also of the access area of the hot fluid in the exchanger is a consequence of the activity of a differentiated concentration cell of the electrolyte.

### *4.2. Corrosion under mechanical stress*

Mechanical stresses that act over a metallic material from a corrosive medium can be: a) tension forces due to external forces implicated in the functioning conditions; b) residual tensions of mechanical, thermal or structural type that appear during the fabrication process (plastic deformation, thermal treatment, welding) or during exploitation (local plastic deformations, temperature variations in the materials with high anisotropy of the thermal dilatation coefficient).

The corrosion under stress takes place in weakly corrosive chemical media and under relatively small mechanical tensions. Thus, for a stainless steel type Cr-Ni-Mo, the risk of corrosion under stress is eliminated if the tensions are kept below 30 % from the flow limit.

The heat exchanger plates contain even from the making process an inhomogeneous state of internal tensions and they are in contact with fluids containing chlorine, which favors the corrosion under stress. We observed at the microscope that the heat exchanger plates present a pitting corrosion of initiation of the trans-crystalline cracks that are specific to corrosion under stress. The developed cracks also prove the evolution of the pitting corrosion and of the branching of the initial crack.

Most cracks begin near the gasket and then propagate into the planar area of the placing position of the gasket, with small tensions, which leads to the conclusion that this corrosion under stress was activated simultaneously with the action of the differentiated aerated cell. Also, the structural inhomogeneities (such as the presence of carbides and the nonmetallic inclusions) of the internal tension field and also the concentration inhomogeneities of the electrolyte (primary and secondary fluids with different temperatures and pressures) have favored the supplementary production of galvanic cells of composition, elastic distortion and of concentration-type, respectively [10].

Because of this complex stress, the 304 AISI steel isn't useful from the chemical composition and from the elaboration point of view, which led to a drastic decrease of the lifetime of our product (the heat exchanger plates).

The corrosion under stress appears at the austenitic stainless steels at the contact area between the steel and the chloride solutions, even at very low concentrations (> 5 ppm chlorine ions) and with very small tension forces. Thus, an austenitic steel type 18Cr – 10Ni suffers a high cracking corrosion in 50 ppm NaCl solutions, at $80^0$ C, under tensions smaller than 1.5 daN/mm$^2$. This phenomenon is also fed by the continuous evaporation of the solution that increases the local chloride concentration and by the thermal shocks that locally destroy the passivating oxide film. The cracks and the corrosion that appear this way have a trans-granular character [8].

## 5. The experimental analysis of the fine structure and the residual tension state

We performed a detailed analysis of our samples at a microstructural level in order to point out some aspects concerning: a) the tensioned state of our material determined by the plastic deformation of the sample; b) eventual structural changes in the material following the stress suffered at the plastic deformation, that can favor the apparition of cracks [3]. We studied the fine structure at the level of the crystalline lattice and the state of residual tensions [12] at the DRON-3 diffractometer (X Cu $K_\alpha$; U = 34 kV; I = 20 mA). The X-ray irradiation scheme is presented in fig. 12 (a – irradiation with a beam perpendicular on the direction of the crack; b – irradiation with a beam parallel with the direction of the crack.

The diffraction spectra of the material from the area unaffected by cracks are presented in figures 13 (according to the scheme from fig. 12a).

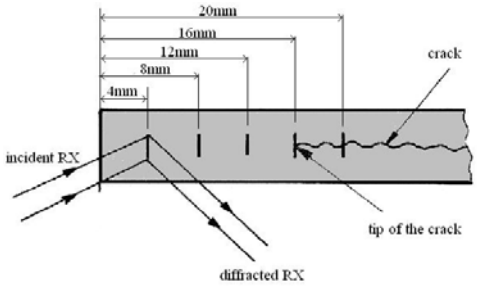


***Fig. 12, a*** *- X-ray irradiation scheme with a beam perpendicular on the direction of the crack*

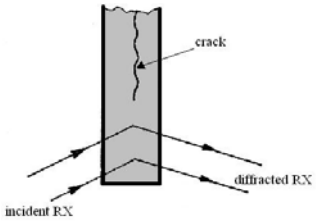


***Fig. 12, b*** *- X-ray irradiation scheme with a beam parallel with the direction of the crack*

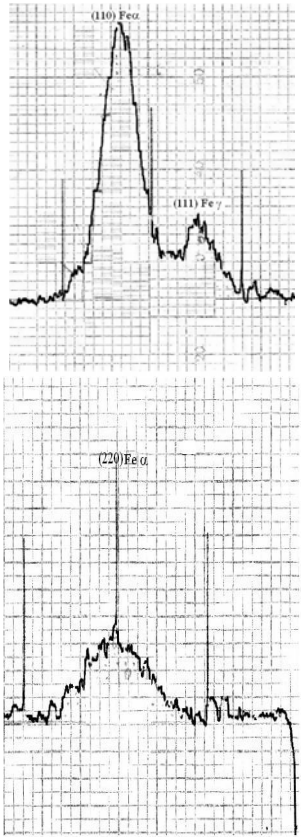


***Fig. 13.*** *X-ray diffraction spectra fragment according to the scheme from fig. 12a*

These spectra fragments inform about the structural states and the tension states from the superficial layer, with a depth of approximately 80 μm

The irradiation schemes we used allowed us: 1) to establish the texturing degree of the material; 2) to get data concerning the 1st order internal tensions that appear at macroscopic level and that are oriented either to stretch, either to compress the material; 3) to get data concerning the 2nd order internal tensions that appear at the level of the mosaic blocks and that are unorientated tensions; 4) to establish the medium size of the mosaic blocks that dictate the breaking tension of the material; 5) to appreciate the density of dislocations from the crystalline lattice that determine the plasticity properties; 6) to make a phase analysis, meaning to determine the martensitic and the austenitic phases and the possible transformation type $Fe_\gamma \rightarrow Fe_\alpha$.

The presented diffraction spectra show the change of form of the diffraction lines for the martensitic and austenitic phases because of the action of the tensions from the areas near the tip of the crack. Their shape proves the existence of a $Fe_\gamma \rightarrow Fe_\alpha$ type of transformation because of the action of the internal tensions. Thus, we concluded that the material is unstable from the structural point of view and this is why the pitting-type of corrosion is favored in the stretched areas of the ply where the fittings are placed. Also, we deduced that the material is inhomogeneous from the texturing degree point of view, thus being favored the structural instabilities at the crystalline grain level, having negative consequences on the corrosion behavior of the heat exchanger plates.

By processing the data from the diffraction spectra we could get a series of important elements such as:

1) The $B_{221}$ magnitude (see fig. 14) is directly proportional with the level of the 2-nd degree internal tensions. From the obtained data we could see that $B_{211}$ increases towards the tip of the crack, thus showing the existence of a tensional inhomogeneity of the material at the level of the mosaic block. This aspect induces the beginning of the pitting corrosion (narrow spaces).

2) The $\Delta_{2\theta}$ magnitude (see fig. 15) is directly proportional with the level of the 1st degree internal tensions. Our results show that towards the tip of the crack there is a tendency that the internal tensions to grow, thus leading to a local stretching process of the material.

These tensions start the transformation of the austenite to martensite, thus influencing the stability of the material.

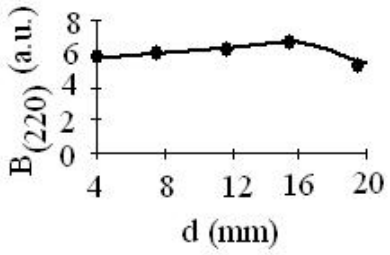


***Fig. 14.*** *The distribution of B (220) size*

The structural stability decreases in time, fact that leads to the beginning and intensifying of the local corrosion process.

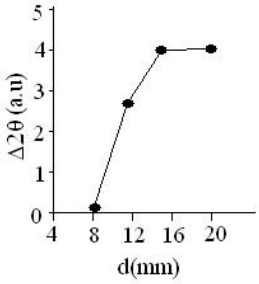


***Fig. 15.*** *The distribution of the $\Delta 2\theta$ magnitude*

3) The $B_{110}$ magnitude (see fig. 16) is directly proportional with the breaking tension of the martensitic phase. The data show that towards the tip of the crack the breaking tension decreases fact that favors the breaking of the martensitic phase from the steel.

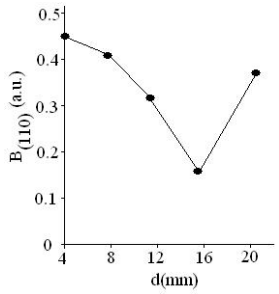


***Fig. 16.*** *The distribution of $B_{110}$ size*

4) The $B_{111}$ magnitude (see fig. 17) is directly proportional with the breaking tension of the austenitic phase. From the data we concluded that towards the tip of the crack the breaking tension decreases, fact that also favors the beginning of the breaking of the material.

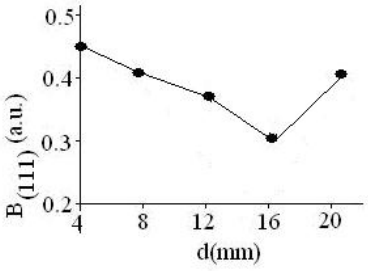


***Fig. 17.*** *The distribution of $B_{(111)}$ size*

5) The $I_{110}$ integral intensity magnitude (see fig. 18) is directly proportional with the quantity of the martensitic phase. This magnitude increases towards the tip of the crack as a consequence of the instability of the martensitic phase caused by the 1$^{st}$ and 2$^{nd}$ degree internal tensions. Thus, the martensitic phase appears, it is metastable and it creates supplementary tensions into the material.

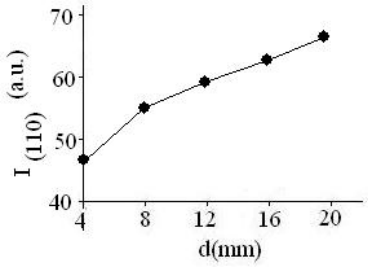


***Fig. 18.*** *The distribution of the integral intensity $I_{(110)}$*

6) The $I_{111}$ integral intensity magnitude (see fig. 19) is directly proportional with the quantity of the austenitic phase. The decrease of the quantity of austenitic phase is done because of its transformation to martensitic phase caused by the action of 1$^{st}$ and 2$^{nd}$ degree internal tensions. The steel looses its austenitic character, becomes martensitic and metastable from the structural point of view.

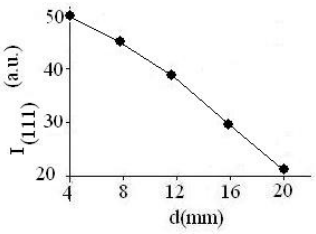


***Fig. 19.*** *The distribution of the integral intensity $I_{(111)}$*

7) The $I_{211}^{min} / I_{211}^{max}$ ratio magnitude (see fig. 20) is proportional with the density of dislocations from the martensitic phase. The decrease of the density of dislocations leads to the decrease of the plasticity properties of the martensitic phase towards the tip of the crack, thus having negative effects over the answer of the material to mechanical stress (stretching or compressing).

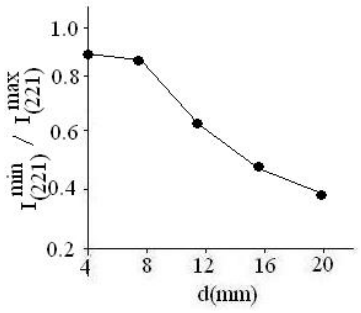


***Fig. 20.*** *The distribution of the* $I_{211}^{min} / I_{211}^{max}$ *ratio*

## 6. Conclusions

The material used for the heat exchanger plates is an austenitic stainless steel with an unstabilized structure due to the presence of inadequate alloying chemical elements.

During the cold plastic deformation process the austenitic phase turned to martensitic phase. This fact determined the apparition of the state of supplementary tensions that overlapped with the residual tension state appeared during the processing of the material.

A lot of nonmetallic inclusions either dispersed or distributed in lines along the rolling direction were observed. We also observed that the material contained plastic formations of sulphures, thus indicating deficiencies concerning the steel making. There is also dispersed and unsolved cementite in the basis mass of the material. This indicates that the material wasn't thermally treated after the cold plastic deformation (hardening in order to be put in solution), which would have led to the diminishing or even to the elimination of the residual internal tensions. Such a treatment would have been indicated for the material used for the heat exchangers.

The first micro cracks accelerated the transformation of the austenite to martensite in front of the crack.

This change provoked a destabilization of the energetic equilibrium by worsening the behavior of the plates to the attack of the liquid medium over the crystalline grains. The elasticity properties of the plate's material decreased and the breaking tension lowered, favoring the propagation of cracks and the destruction of the plate. This process of developing of micro cracks and of their change to macro cracks, followed by their propagation is favored by the lack of material stabilization.

The cracks initiated at the surface of the material and having an obvious tendency of branching in depth and in plane are specific to the cracking corrosion under stress. This type of corrosion takes place even if the tensions from the material are relatively small compared to the limit of resistance of the steel, as the computer simulation showed us.

Because the plates of the heat exchangers have a complex shape, they have to be realized by cold plastic deformation. As a consequence, the microhardness increases, as we could notice at the analysis of microhardness we made.

The material is softer in the relaxed areas very close to the crack. The analysis made in cross-section showed a bigger hardening on the stretched part of the material then on the compressed part, which favored the propagation of cracks both in depth and on the plane part of the plates. The growth of hardness is favored by the partial transformation of the austenite to martensite caused by the instability of the structure of the material. One has to also keep into account that the martensite is harder than the austenite.

The analysis of the microhardness also showed that there is a hardening of the material at the edge of the plate due to the cutting of the semi fabricated as a metal sheet. This fact confirms that there wasn't done any thermal treatment during processing.

The absence of structural stability and the presence of residual tensions from the cold plastic deformation lead to the formations of deep craters of pitting-type in the material, even in low corrosive media. From these craters begin the transcrystalline cracking. We consider that this process is favored by the simultaneous action of more factors, such as:

- the presence of oxygen solved in the liquid medium;
- the higher temperature at the inlet of the primary thermal agent;
- the diminished circulation of the thermal agent in the area towards the exterior part of the heat exchanger plate;
- a possible aggressive action of the unlinked sulphur from the material of the fittings that, in time, can enter the metallic material, this process being favored by the higher temperature;
- the appearance of differentiated composition cells in the contact area between the gaskets and the plate, towards the exterior corner, opposite to the main flowing direction of the working fluid, thus favoring the corrosion process of the used steel.

Taking into account the processing and the functioning conditions of the material, we consider that it would have been better to use for the heat exchanger plates a stainless steel with stabilized structure, by adding molybdenum. Such steel is 316 AISI, which contains 2 – 3 % Mo (molybdenum).

## References

**[1]. Gheorghies,** 1990, C. *Controlul structurii fine a materialelor cu radiatii X*, Ed. Tehnica, Bucuresti, p 272
**[2]. He, S., Jiang, P.X., Xu, Y.J., Shi, R.F., Kim, W.S. and Jackson**, J.D., Int. J. Therm. Sci., 2005, vol. 44(6), pp.521-530.
**[3]. Satake, S., Kunugi, T., Shehata, A. M. and McEligot, D. M**., 2000, Int. J. Heat Fluid Flow, 21, pp. 526-534.
**[4]. Lours, P., Huchet, L.,** 2001, Analyse d'avaries de pieces metalliques, Ecole des Mines d'Albi-Carmaux, France.
**[5]. Stephen, A. J**., 2003, International Journal of Heat and Fluid Flow, vol. 24, Issue 6,
**[6]. Kim, W. S., Jackson, J.D., He S. and Li, J**., 2004, Journal of Mechanical Engineering Science, vol. 218, pp. 1361-1372.
**[7].** STAS 3583-87
**[8].** STAS 7657-78
**[9]. Lucan, D., Pirvan, I., Radulescu, M., Fulger, M., Jinescu,G.,** 1998, Revista de chimie vol. 49, pp. 222 -226
**[10].** STAS 7114/1991
**[11]. Vukoslavcevic, P., and Wallace, J. M**., 2001, 54th Annual Meeting, San Diego, USA, November. *Bull., Amer. Phys. Soc.*, 46 (No. 10), p. 89.
**[12]. Gheorghies, C**., 2003, The Ann. of Dunarea de Jos Univ. of Galati, Fasc. VIII, Tribology, vol.I, pp.302-312.